Poly-L-Lysine-Induced Morphology Changes in Mixed Anionic/Zwitterionic and Neat Zwitterionic-Supported Phospholipid Bilayers

Tighe A. Spurlin and Andrew A. Gewirth
Department of Chemistry, University of Illinois at Urbana-Champaign, Urbana, Illinois 61801

ABSTRACT Poly-L-lysine-induced morphological changes in liquid phase supported bilayers consisting of mixed anionic/zwitterionic and neat zwitterionic headgroup phospholipids were studied with atomic force microscopy and epifluorescence microscopy. Results obtained from these studies indicate that poly-L-lysine can induce domains, defects, and aggregate structures on both mixed bilayers and strictly zwitterionic bilayers. The structures formed on liquid phase supported bilayers were observed to be immobile from a timescale of 50 ms to several minutes. We propose that poly-L-lysine of sufficient length interacts with the mica substrate and phospholipids to create the stationary structures noted.

INTRODUCTION

Supported phospholipid bilayers and unilamellar vesicles are used as models for cell membranes. The interactions between lipid membranes and both synthetic polymers (1–3) and isolated natural proteins (4–6) with these constructs are studied to gain insight into complex processes occurring at cell membranes. Several reviews cover the utility of using supported bilayers to model processes occurring at more complex cell membranes (7,8). Unilamellar vesicles of various sizes are also used to model cell membranes (9–11). Studies on vesicles offer the advantage of being independent of substrate-induced effects, such as asymmetric diffusion in the inner and outer leaflets (12) and lipid distribution asymmetries (13,14). However, the stability of supported bilayers (8) offers the advantage of using methods such as attenuated total reflectance infrared spectroscopy (15), neutron scattering (16), and atomic force microscopy (AFM) (17), which are sometimes more difficult to use with the unilamellar vesicles. Additionally, experimental results on vesicles exhibiting transmembrane symmetry do not match conditions present at cellular membranes. Several studies have determined that lipid distribution asymmetries (18–20), differences in inner/outer leaflet viscosities (21,22), and phase-separated domains may not exist as transmembrane domains (23) due to cytoskeleton proteins (19) and/or a variety of translocase enzymes (18). Therefore, a variety of experimental designs is required to provide valuable insight into ways in which polymers, proteins, and lipids organize into more ordered domains, insert into/across lipid membranes, and even disrupt lamellar packing by forming lipid aggregates. The details of the ways in which proteins or other polymers cause organization and other constructs are not fully understood.

Cell membranes are thought to contain both disordered fluid phase lipids and more ordered fluid phase lipids, which coexist in the membrane as separate domains (24–26). Fluid phase lipids in cell membranes are thought to form ordered fluid phases through interactions with cholesterol, sphingomyelin, gangliosides, and a variety of proteins (24,25,27). The size of ordered fluid phase lipid domains formed from these interactions has not been definitively determined. Literature values for ordered lipid domains in cells have ranged from $<$70 nm to 300 nm (28,29), and studies using model systems reported domain sizes of several microns (25). Additionally, the percentage of ordered fluid phase lipids in cell membranes published varies widely from 13% to 50% (24,30). Even with questions about the dimension and structure of liquid ordered domains remaining, experimental evidence has implicated ordered fluid phase domains in important cell role functions, such as membrane trafficking and membrane signaling (26).

Dysfunctions in the organization of lipids in cell membranes are linked to serious disorders, such as Tay-Sachs, Fabry, and Sandhoff disease (31–33). The topic of ordered lipid domains is typically covered from the perspective of cholesterol-sphingolipids-phospholipid interactions. However, protein-lipid domains have also been observed (32,34–36) to form through electrostatic (1,34,35) and nonelectrostatic (37–39) interactions. Domains formed from protein-lipid interactions may be involved in phagocytosis, exocytosis, and membrane trafficking (34,40–42). Therefore, a better understanding of protein-lipid domain formation is essential to understanding cell function and dysfunction.

Model polypeptides, such as poly-L-lysine (PLL), provide an excellent opportunity to examine phospholipids-polypeptide interactions. PLL is used as a model for natural peripheral proteins containing positive charge, such as myrisotylated alanine-rich C kinase substrate (34). Shorter polylysine chains consisting of four to six units and longer chain polylysine with 30 or more lysine units are thought to exist in solution as random coils (43). However, upon

Submitted February 1, 2006, and accepted for publication July 5, 2006.

Address reprint requests to Andrew A. Gewirth, Dept. of Chemistry, University of Illinois at Urbana-Champaign, 600 South Mathews, Urbana, IL 61801. Tel.: 217-333-8329; Fax: 217-333-2685; E-mail: agewirth@uiuc.edu.

0006-3495/06/10/2919/09 $2.00

doi: 10.1529/biophysj.106.082479

binding to a phospholipid bilayer the longer chain polylysine adopts a α-helix form when phosphatidylserine (44) or phosphatidylglycerol (45) headgroups are present and a β-sheet form in the presence of phosphatidic acid headgroups (46), whereas the short chain retains a random coil form.

Substantial effort has been directed at understanding the interplay between PLL and phospholipid bilayers (3,34,35, 47–50). However, the exact nature of this interaction is still under debate, especially in the case of lipid bilayers composed of zwitterionic lipid headgroups and mixed zwitterionic/anionic headgroups. For example, fluorescent microscopy data showed that both short chain (34) and long chain PLL (49) may form domains enriched in anionic lipids, whereas similar studies (35) with NMR conclude that shorter chain polylysine did not form domains. More recent results (49) suggest that both short chain polylysine and long chain PLL first create domains in a lipid bilayer and then creates defects in the bilayer which allows aggregated PLL-lipid ropes to enter. The ongoing debate concerning the interaction of short and long chain polylysine with both zwitterionic and mixed zwitterionic/anionic lipid bilayer warrants further investigation. The importance of this topic is severalfold considering that PLL enhances the delivery of DNA across cell membranes (3), increases the effectiveness of certain classes of drugs (50), and that lysine residues play an important role in eukaryotic antimicrobial responses (4).

This study utilizes AFM and fluorescence microscopy to interrogate the changes long chain polylysine ($n \sim 100$) generate in supported phospholipids bilayers consisting of either pure zwitterionic lipids or a mixture of zwitterionic and anionic lipids. AFM was utilized to determine changes in the supported bilayer morphology over time as PLL adsorption occurred. Fluorescence microscopy was carried out to identify lipids involved in morphological changes observed in AFM experiments.

MATERIALS AND METHODS

Phosphate buffers (10 mM, pH = 6.4) with 150 mM sodium chloride were prepared with ultrapure, 18.2 MΩ cm, water (Milli-Q UV plus, Millipore, Billerica, MA) using reagents of >99% purity. 1,2-dimyristoyl-*sn*-glycero-3-phosphcholine (DMPC), 1,2-dipalmitoyl-*sn*-glycero-3-phosphcholine (DPPC), 1,2-dioleoyl-*sn*-glycero-3-phosphcholine (DOPC), 1,2-dioleoyl-*sn*-glycero-3-phosphserine (DOPS), 1-oleoyl-2-[12-[(7-nitro-2-1,3-benzoxadiazol-4-yl)amino]dodecanoyl]-*sn*-glycero-3-phosphoserine (NBD-DOPS) were purchased from Avanti Polar Lipids (Alabaster, AL) and used without further modification. Long chain PLL (MW ~15,000–30,000) with an average DP of 103 was obtained from Sigma-Aldrich (Milwaukee, WI).

Supported bilayer formation

Phospholipids dissolved in chloroform were added to a round bottom flask in the appropriate amounts, dried under argon gas, and kept under vacuum overnight to remove trace amounts of chloroform. The lipid film obtained from drying was then hydrated in the desired buffer for at least 2 h above the lipid phase transition with periodic mixing to form multilamellar vesicles. Vesicles were then extruded above the lipid phase transition through polycarbonate membranes containing 100-nm pores to form small unilamellar vesicles (Avanti Polar Lipids).

Supported bilayers were formed on either cleaved mica for AFM experiments or quartz for fluorescent studies through the incubation of unilamellar vesicles at a concentration of 1 mg/ml in a solution cell for a least 1 h above the lipid phase transition temperature. Previous workers showed that lipid bilayers composed of up to 25 mol % DOPS form on mica substrate (51) and silica substrates (52). Rinsing with buffer was performed after bilayer formation to remove excess vesicles from the solution cell. During the rinsing procedure the bilayer must not be exposed to air or the supported bilayer will become extremely defected due to lipid loss from the surface. The fusion of vesicles with similar composition to solid supports has been shown previously (53,54). Supported bilayers are thought to be separated from the substrate by a layer of water (~1–2 nm). However, the substrate has been shown to affect the lipid melting transition (55–57), so care was taken to establish bilayers in the gel and fluid states by AFM temperature ramping. Unless otherwise stated, PLL was incubated over the substrate for 1 h, after which time PLL-free buffer was utilized to remove any free PLL that remained in solution.

Fluorescence microscopy

Quartz microscope slides (Esco, Oak Ridge, NJ) used for fluorescent studies were cleaned in piranha solution for 1 h and then copiously rinsed with Milli-Q water. Immediately after Milli-Q rinsing, a Teflon o-ring and cell were clamped onto a slide and filled with a buffer solution to preserve substrate cleanliness. Supported bilayers were prepared on clean microscope slides as described in the previous subsection. After vesicle incubation, fluorescent images were taken after rinsing with buffer to check bilayer integrity within the resolution limitations of the objective.

An Axiovert 200 microscope (Carl Zeiss, Oberkochen, Germany) with an air objective (numerical aperture 0.7) and Ixon charge-coupled device camera (Andor, South Windsor, CT) were used as an epifluorescence microscope to collect images of supported bilayers. A 50-mW laser (Crystal Laser, Reno, NV) operating at a wavelength of 532 nm was passed through a filter to decrease the intensity to ~5 mW before being utilized to excite fluorescently labeled phospholipids. DOPS lipids labeled with nitrobenzoxadiazol (NBD) in the hydrocarbon chains were utilized as fluorescent probes. Data analysis was performed using Andor Ixon software.

Atomic force microscopy

Supported bilayers were created on freshly cleaved mica through the vesicle fusion technique outlined above. A PicoSPM 300 (Molecular Imaging, Tempe, AZ) equipped with a Type D scanner controlled by a Nanoscope E controller (Digital Instruments (now Veeco) Fremont, CA) was operated in magnetic acoustic (MAC) mode during imaging. Type II Maclevers (Molecular Imaging) with a resonant frequency of 22–25 kHz in aqueous solutions and a spring constant of ~2.8 N/m were driven through the use of a solenoid attached to the bottom of a sample stage (Molecular Imaging). The sample stage could also be utilized to control the temperature ($\pm$0.1 C), when necessary, during image collection through an ice water cooling system, Peltier device, and cryogenic temperature controller (Lake Shore Cryogenics, Westerville, OH). AFM images were collected with a scan rate of <2 Hz and 512 $\times$ 512 pixel resolution. Data analysis was carried out using Nanoscope E version 4.23 (Digital Instruments) and WSxM version 3.0 (Nanotec Electronica S.L., Madrid, Spain).

RESULTS AND DISCUSSION

AFM measurements

The first set of AFM measurements focuses on observing the morphology changes PLL causes in mixed bilayers composed

of 10 mol % DOPS and 90 mol % DOPC. The goal of these experiments was to observe domains formed between PS lipids and PLL, which previous studies have observed with fluorescent (49) and NMR (35) techniques. In addition to domain formation we utilized AFM to check for other morphology changes.

Fig. 1 *A* shows 10 × 10 μm MAC mode AFM images of a 10 mol % DOPS/90 mol % DOPC bilayer obtained at 25°C—a temperature well above the gel to fluid phase transition of both DOPC (−20°C) and DOPS (−11°C) (58)—before addition of PLL. The image is featureless with no evidence of domains or defects, consistent with previous AFM images of fluid phase supported bilayers (55,59,60). Confirmation of bilayer formation on the mica support was obtained through thickness measurements of deliberately damaged bilayers. The thickness obtained for 10 mol % DOPS/90 mol % DOPC was 3.8 ± 0.5 nm, which is similar to that found in previous work (51,61).

Fig. 1 *B* shows an AFM image obtained at 25°C after addition and incubation of 125 μM PLL followed by rinsing with PLL-free buffer. The figure shows the clear presence of domains, defects, and aggregates. Fifteen defects—two of which are marked with a white line—were analyzed using cross sectional analysis and were found to be 3.9 ± 0.5 nm in depth, which is within the error for the bilayer thickness before PLL addition. Artifacts arising from tip-substrate interaction are also seen, but the image was stable to repetitive scanning. Scanning different 10 × 10-μm areas of each sample after PLL addition resulted in images similar to that in Fig. 1 *B* and indicates that the changes in morphology were not localized events.

To better visualize domains and defects and to aid in height analysis, images were captured at higher magnification (5 × 5 μm) as shown in Fig. 1 *C*. The images show the presence of a domain of material—marked with a white line—formed above the bilayer in addition to the defects—marked with a white star in Fig. 1 *C*—previously mentioned. Cross section analysis of 20 domains gave a height above the bilayer of 0.6 ± 0.3 nm. This height is reasonable as groups have reported polymers (62,63), such as DNA, which reside 0.7 ± 0.2 nm above fluid phase bilayers. Multiple measurements showed that the domains occupied ~8% ± 4% of the surface, whereas defects occupy ~1.7% ± 1% of the surface.

Increasing the concentration of PLL to 600 μM in the sample cell increased the domain coverage to ~39% ± 10% as shown in Fig. 1 *D*. The increased domain coverage with increased PLL concentration confirms that PLL must be inducing domain formation because other experimental variables remain unchanged. Additionally two other features were occasionally observed with addition of 600 μM PLL. First, material exhibiting heights above the bilayer of 5.4 ± 0.5 nm seen on isolated regions of the bilayer are apparent multilamellar stacks. Second, some samples exhibited spherical aggregates 1.8 ± 0.8 nm above the bilayer, an example of which resides inside the star on Fig. 1 *E*.

To show that the morphology changes seen in Fig. 1, *B–E*, were due to lipid-PLL interactions and not simply aggregated PLL on mica, we performed a control study. Fig. 1 *F* proves that incubating 600 μM PLL over freshly cleaved mica does not result in the structures seen in 10 mol % DOPS/90 mol % DOPC studies. Additional control studies undertaken with 125 μM PLL provided identical results. Thus, AFM data show that long chain PLL can create defects, domains, aggregates, and—in isolated instances multilamellar—stacks in DOPS/DOPC.

Our AFM images are similar to previous results obtained (49) with comparable lipid compositions and indicate that PLL adsorption to giant unilamellar vesicles removed both PS and PC headgroup lipids from the bilayer leaflets. The unsupported vesicles were observed (49) to have lipid-PLL

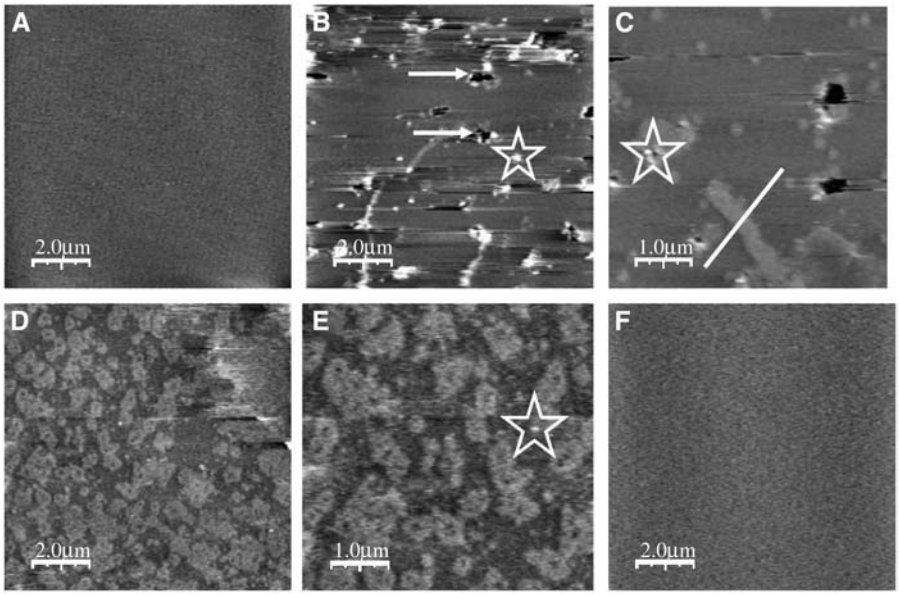

FIGURE 1 (*A*) Pure 10 mol % DOPS/90 mol % DOPC. (*B–C*) After addition of 125 μM PLL. (*D–E*) After addition of 600 μM. *F* 600 μM PLL added to mica alone. Arrows point to defects revealing the mica substrate. Stars highlight spherical aggregates, and a line is used to denote PLL-induced domains.

aggregates present both inside and outside the giant unilamellar vesicles.

To evaluate the role of the anionic DOPS component in defect and domain formation in the presence of PLL, we examined the interaction of PLL with neat DMPC or DPPC bilayers. Both DMPC and DPPC are zwitterionic. Before each measurement, bilayers were imaged in the gel phase and the temperature ramped through the phase transition to be certain PLL was added to fluid bilayers. Starting experiments in the gel phase provided verification of bilayer formation through thickness values of 4.6 ± 0.5 nm for DMPC and 5.5 ± 0.4 nm for DPPC taken from defects similar to those marked with arrows in Fig. 2 *A* that exposed the mica substrate. The temperature of the sample stage was increased to observe the phase transition of DMPC and DPPC. At temperatures higher than the phase transition temperature fluid phase bilayers with uniform morphology as indicated by Fig. 2 *B* were seen as expected (55,60).

Addition of 100 μM PLL to DMPC shown in Fig. 2 *C* or 50 μM PLL to DPPC shown in Fig. 2 *D* results in a dramatically different fluid phase morphology exhibiting upraised aggregates and defects. Defects spanning the bilayer, highlighted in Fig. 2 *C*, through the use of a line, observed in fluid phase DMPC bilayers provided a thickness value of 3.3 ± 0.4 nm. Defects pictured in Fig. 2 *D* for fluid phase DPPC bilayers were 4.4 ± 0.4-nm deep. These thickness values for DMPC and DPPC suggest that even after exposure to PLL the bilayer is still in the fluid phase (59,64). Additional evidence that the bilayer remained in the fluid phase was garnered from temperature-ramping studies acquired after PLL adsorption, which showed that a phase transition at ~23°C was still present. The upraised aggregates, one example of which is marked with a star in Fig. 2, *C* and *D*, exhibited heights above the bilayer of 8.5 ± 4.5 nm and 10.1 ± 6.3 nm above the bilayer for fluid DMPC and fluid DPPC bilayers, respectively. After observing the morphology change in fluid bilayers upon PLL addition, the samples were cooled into the gel state.

Fig. 2, *E* and *F*, provides representative images of gel phase DMPC and DPPC bilayers after PLL addition, respectively. The gel bilayer thickness after PLL addition was relatively unchanged at 4.7 ± 0.4 nm for DMPC and 5.2 ± 0.4 nm for DPPC as measured from cross section analysis of defects extending to the mica substrate, as illustrated by lines in Fig. 2, *E* and *F*.

PLL interaction with zwitterionic lipids seems to be a more contentious point in the literature with simulations (4), fluorescent microscopy (49), and infrared spectroscopy (47,65) showing interaction, whereas other studies suggest no interaction between neutral lipid headgroups and PLL (35,46). A related AFM study (66) directly observed defect formation in fluid phase DMPC bilayers caused by protonated amine terminated PAMAM dendrimers-zwitterionic lipid interactions. The formation of aggregates and defects on zwitterionic bilayers observed in our AFM images show that PLL is capable of interacting and disrupting the bilayer.

Fluorescence measurements

AFM results indicate that long chain PLL does interact with zwitterionic PC lipids in both the gel and fluid states. We used fluorescent tagging methods to further investigate DOPS segregation into domains with the presence of PLL. Due to the difficulty of forming pure DOPS bilayers on mica surfaces due to electrostatic repulsion (67), we examined a mixed bilayer system. Bilayers were prepared with 0.1 mol % NBD-tagged DOPS, 9.9 mol % DOPS, and 90 mol % DOPC on a quartz substrate to visualize domains containing

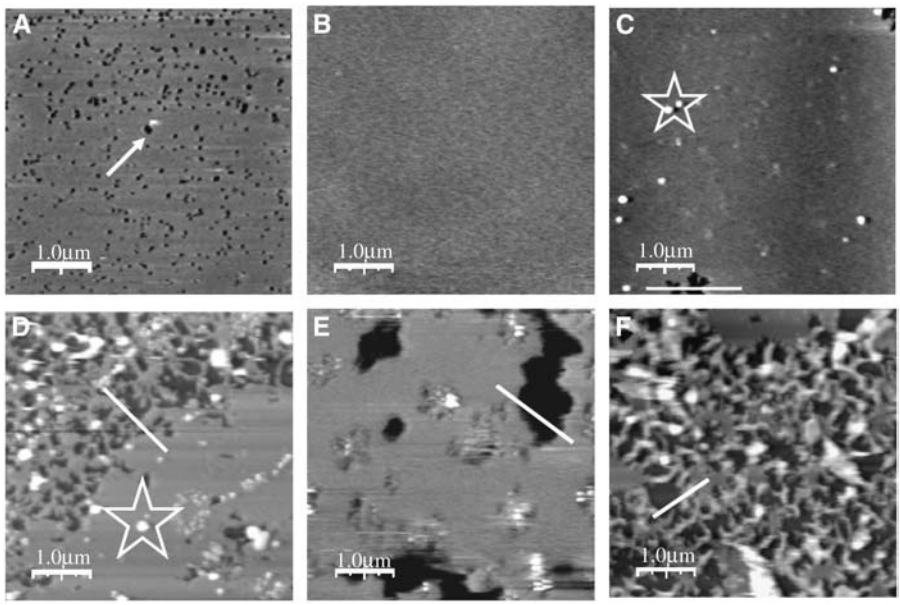

FIGURE 2 (*A*) DMPC gel phase. An arrow points to a defect extending to the mica substrate. (*B*) DMPC liquid phase. (*C*) Liquid phase DMPC after addition of 50 μM PLL. A star encircles two spherical aggregates. (*D*) Liquid phase DPPC after addition of 50 μM PLL. A line is drawn over a defect, and a star is used to denote a spherical aggregate. (*E*) DMPC cooled from liquid phase to gel phase after 50 μM PLL addition. A line is drawn over a defect. (*F*) DPPC cooled from liquid phase to gel phase after 50 μM PLL addition. A line is drawn over a defect. (*A*, *E*) 15°C. (*C*) 45°C. (*D*) 56°C. (*F*) 24°C.

PS headgroups with fluorescent microscopy. Fluorescence imaging was performed with the bilayer in the fluid phase.

Fig. 3 *A* shows that clean quartz substrates under phosphate buffer saline (PBS) buffer do not produce a fluorescence signal, as expected. Upon adding lipid vesicles to the solution cell the bulk solution fluoresced indicating NBD-DOPS was incorporated into the vesicles. After vesicle incubation the solution cell was rinsed with PBS buffer to remove all vesicles from solution, leaving a uniformly fluorescent supported bilayer on the quartz substrate as indicated by Fig. 3 *B*. This procedure ensures that any domains seen are the result of PLL interactions with the supported bilayer and not PLL interactions with vesicles in solution. As seen in Fig. 3 *C*, and pointed out by arrows, the addition of 100 μM PLL results in a bilayer that is no longer uniformly fluorescent and contains small regions of higher fluorescent density.

To be certain that PLL itself did not contain fluorescent moieties which caused the nonuniform fluorescent spots seen in Fig. 3 *C*, we incubated 100 μM PLL in PBS over a quartz substrate. Fig. 3 *D* proves that PLL does not produce any fluorescent signal on the quartz surface. Thus, the bright spots in Fig. 3 *C* are DOPS molecules segregating into domains upon PLL addition because these are the only fluorescent molecules excited by the laser source present in the system. These results are similar to previous fluorescent studies on giant unilamellar vesicles with both short chain PLL (34) and long chain PLL (49), which suggest that PLL interacts with DOPS to form domains.

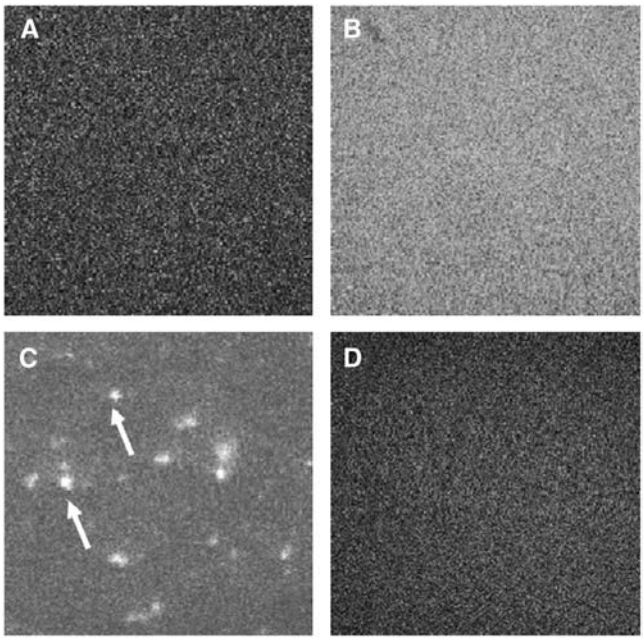

FIGURE 3 (*A*) Control study PBS buffer over quartz. (*B*) Image of 0.1 mol % NBD-DOPS/9.9 mol % DOPS/90 mol % DOPC. (*C*) 100 μM PLL solution over DOPS/DOPC bilayer. Arrows point to bright fluorescent spots, indicating NBD-DOPS segregation. (*D*) Control study 100 μM PLL in PBS over quartz. All Images are 50 $\times$ 50 μm.

Determining PLL-lipid domain diffusion with AFM and fluorescence

The fluorescent microscope utilized also provided a method to capture movies of the DOPS/DOPC bilayer with PLL adsorbed to determine if domains diffused. In these studies, the region of the bilayer with domains induced by PLL addition had 100 images at a capture rate of 50 ms taken for a total capture time of 5 s. The image shown in Fig. 4 *A* is the first frame of one of the movies collected showing domain formation and is labeled as time (*T*) equals zero. The next two images, Fig. 4, *B* and *C*, respectively, show the 50th movie frame ($T = 2.5$ s) and 100th movie frame ($T = 5$ s). A visual comparison of nonuniform spots highlighted with arrows in Fig. 4, *A–C*, leads to the conclusion that these domains are not diffusing over 5 s.

To determine if domains may diffuse over longer periods of time, AFM images of the same region were scanned at various time intervals. The images shown as Fig. 4, *D* and *E*, were captured 10 min apart and show no visible change in domain position. To be certain that the domains had not moved, distances between domains were measured with the cross section analysis tool over several regions of the image as illustrated by the line in Fig. 4, *D* and *E*. The distance between domains measured from Fig. 4 *D*, represented as a plot of black squares in Fig. 4 *F*, was compared to the cross section, plotted as gray squares in Fig. 4 *F*, from Fig. 4 *E* that was taken 10 min later. The cross sectional overlay depicted in Fig. 4 *F* indicates that no apparent change in domain location was observed as the cross sections denote high correlation. Repetition of this procedure between several domains shown in Fig. 4, *D–F*, and other samples resulted in lateral distance changes between domains not exceeding 25 nm over a timescale of 10 min. This value represents just over 1% of the size of the scan and is close to the estimated error.

AFM and fluorescent images suggest that over a range of milliseconds to minutes PLL-induced domains do not diffuse in the lipid bilayer. Thus, we can conclude that PLL adsorption to supported bilayers produce domains that are restricted to one location.

The lack of domain diffusion in the fluid bilayer is evidence that the positively charged PLL inserts across the lipid bilayer to interact with the negatively charged mica substrate. The estimated length of the PLL used in these experiments is ~15 nm, assuming that 1) the PLL assumes an α-helix structure, and 2) the lysine monomer length is ~0.15 nm. Therefore, PLL could span the hydrophobic core of any of the bilayers used with the thickest bilayer being DPPC at 5.5 nm. Precedent for PLL insertion across giant unilamellar vesicles exists in the literature (49,68) suggesting that PLL would also be able to cross supported bilayers. The fluorescent microscopy results shown in Fig. 4 eliminate the possibility that the AFM tip induces PLL translocation (62) through the observation of immobile domains in tip independent measurements.

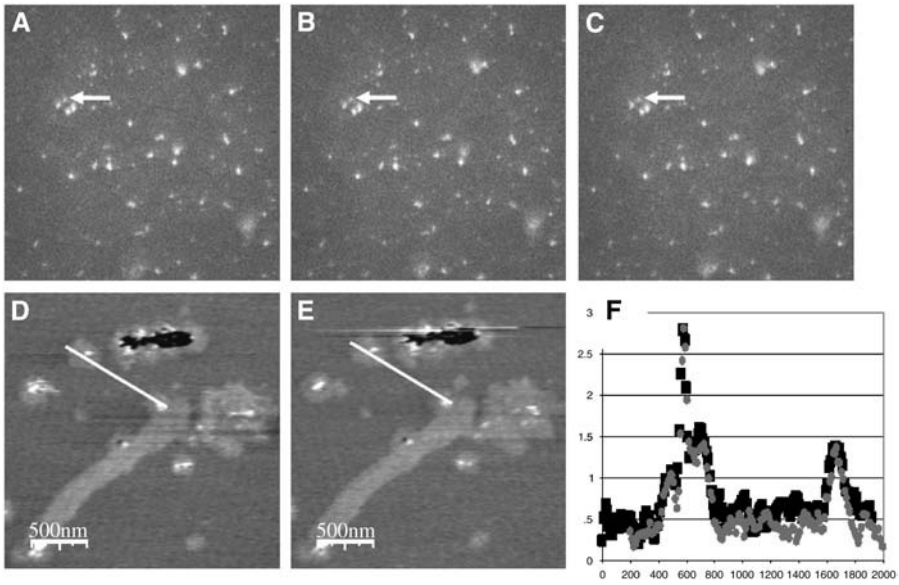

FIGURE 4 (*A*) $T = 0$ after 100 μM PLL addition. (*B*) $T = 2.5$ s after 100 μM PLL addition. (*C*) 5 s after 100 μM PLL addition. (*D–E*) AFM images taken 10 min apart. (*F*) Cross section analysis of domain movement in AFM images. Arrows in panels *A–C* illustrate that the bright fluorescent spots representing segregated NBD-DOPS are immobile. Lines in panels *D–E* represent cross section comparisons which are shown in panel *F*. Panels *A–C* are select fluorescent images from a movie of 100 frames with a capture time of 50 ms. Fluorescent image size is 100×100 μm. AFM image size is 2×2 μm.

PLL changes to bilayer morphology over time observed with AFM

After AFM and fluorescent experiments, which indicate PLL interacts with both anionic and zwitterionic lipids, AFM was utilized to observe the morphology changes over time in an attempt to gain a better understanding of domain formation and lipid loss from the surface. In these experiments a lipid bilayer was formed and equilibrated in the liquid phase before PLL was added to the solution cell and images were collected over time.

Fig. 5 *A* depicts a 10 mol % DOPS/90 mol % DOPC bilayer 5 min after PLL addition in which domains, highlighted with an arrow, were observed immediately. The streaks in Fig. 5 *A* are most likely due to PLL adsorbing or interacting with the tip and being removed because subsequent images, as illustrated by Fig. 5 *B*, of the same area do not show these features. Alternatively these features could be caused by some transient interaction between PLL and the bilayer that the scanning AFM tip could not resolve due to the slow 2-Hz scan rate. Fig. 5 *B* shows the same spot after 40 min to demonstrate that no additional domain formation occurred. Fig. 5 *C* taken at higher magnification clearly shows a heterogeneous surface with various size domains. The domains resided above the bilayer 0.8 ± 0.3 nm from cross sections as indicated by the line in Fig. 5 *C*. As expected, the domain height was similar to that found after 1-h incubation studies. Likewise, defects extending to the mica surface found in isolated sections of the bilayer had a depth of 3.8 ± 0.6 nm as reported in the previous section describing AFM measurements.

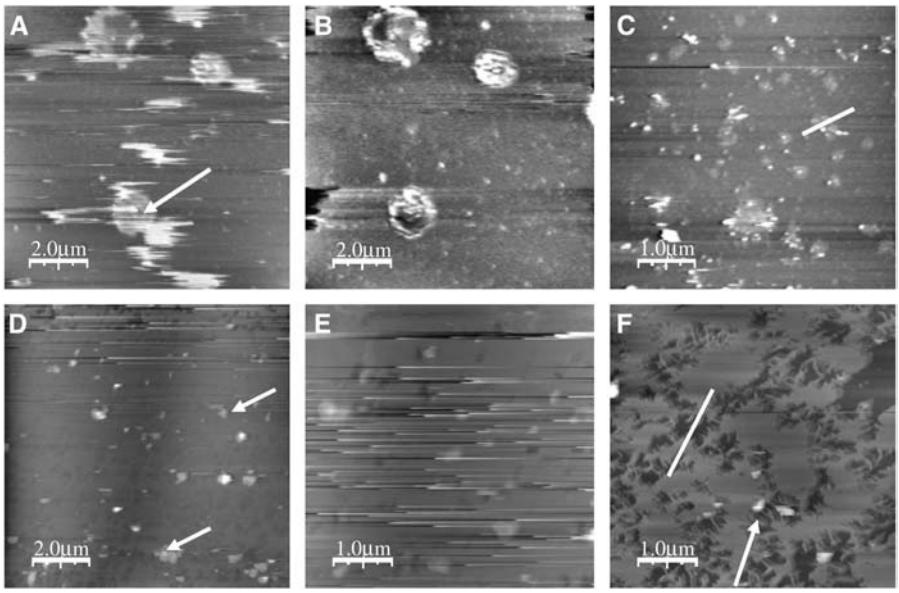

FIGURE 5 (*A*) Five minutes after PLL addition. An arrow points to a PLL-induced domain. (*B*) Forty minutes after PLL addition. (*C*) Magnified image after PLL incubation. The line represents a cross section over a PLL domain. Images *A–C* of 10 mol % DOPS/90 mol % DOPC bilayer. (*D*) Five minutes after PLL addition. Arrows point to domains formed. (*E*) Twenty minutes after PLL addition. (*F*) Forty minutes after PLL addition. A line spans a defect formed in the bilayers, and an arrow points to a spherical aggregate seen.

Adsorption of PLL to a fluid phase zwitterionic DPPC bilayer over time was also observed with AFM. Images captured at 5 min showed domains—pointed out by arrows in Fig. 5 *D*—that resemble those seen in the mixed bilayer experiment. As in the mixed bilayer case the scan obtained 20 min after PLL addition, shown in Fig. 5 *E*, also shows either tip interactions with the surface or transient events leading to lipid loss from the surface. Fig. 5 *F* shows an image obtained 40 min after PLL addition exhibiting no upraised domains. Additional scans collected away from the initial area showed an equivalent defect structure, indicating that tip-sample interactions are not solely to blame for the removal of lipid material. No further changes in morphology were observed through 60 min. At the end of the 40-min liquid phase DPPC bilayers were highly defected, which allowed a bilayer thickness of 4.1 $\pm$ 0.5 nm to be obtained relative to the mica substrate from cross section analysis as indicated by the line in Fig. 5 *F*. Aggregates residing 10.1 $\pm$ 6.3 nm above the DPPC bilayer surface were also observed and pointed out through the use of an arrow in Fig. 5 *F*.

The time-dependent adsorption studies indicate that PLL adsorbs to both mixed anionic/zwitterionic and zwitterionic phospholipid bilayers within 5 min but that additional changes in morphology occur over at least 40 min. In the case of 10 mol % DOPS/90 mol % DOPC bilayers, the morphology changes include the loss of some lipid from the surface and an increase in the amount of surface covered by domains. However, for zwitterionic DPPC bilayers it seems that aggregates form over time and greater amounts of lipid are lost from the surface.

During the first 5 min, PLL likely adsorbs to the supported bilayer from a random coil in solution to form α-helices on the bilayer surface as has been shown (43,44). Within the first 5 min adsorbed PLL must also translocate across the bilayer using defects already present in the bilayers (69–72) or defects created through PLL-induced lipid removal (49,66,73), as some domains/aggregates highlighted in Fig. 5, *A* and *B*, of 10 mol % DOPS/90 mol % DOPC and Fig. 5, *D* and *E*, of DPPC fluid bilayers do not move.

CONCLUSION

The results of this study show that long chain PLL ($\sim$100 residues) can form domains, defects, and aggregate structures on both mixed bilayers containing the anionic lipid DOPS and pure zwitterionic bilayers. Once formed, the PLL-induced structures were observed to be immobile on the timescale from 50 ms to several minutes in images obtained with fluorescent microscopy and AFM.

We propose that after PLL adsorbs from solution to the supported bilayer that PLL either creates defects in the bilayer through lipid removal or inserts through unresolved small defects to interact with the substrate. The interaction of PLL with the mica substrate is believed to create the immobile domains observed in captured images. Morphological changes observed in these model-supported bilayer studies may be similar to changes observed in cell membranes that allow ions, drugs, and even DNA to cross into the cell.

The authors thank Liangfang Zhang and Professor Steve Granick for assistance with fluorescence microscopy results.

This work was supported by the U.S. Department of Energy, Division of Materials Science, under Award No. DEFGO2-91ER45439 through the Frederick Seitz Materials Research Laboratory at the University of Illinois at Urbana-Champaign. T.A.S. acknowledges the Department of Chemistry for financial support.

REFERENCES

1. Murray, D., A. Arbuzova, G. Hangyas-Mihalyne, A. Gambhir, N. Ben-Tal, B. Honig, and S. McLaughlin. 1999. Electrostatic properties of membranes containing acidic lipids and adsorbed basic peptides: theory and experiment. *Biophys. J.* 77:3176–3188.
2. Xie, A. F., and S. Granick. 2002. Phospholipid membranes as substrates for polymer adsorption. *Nat. Mater.* 1:129–133.
3. Fischer, D., Y. Li, B. Ahlemeyer, J. Krieglstein, and T. Kissel. 2003. In vitro cytotoxicity testing of polycations: influence of polymer structure on cell viability and hemolysis. *Biomaterials.* 24:1121–1131.
4. Kandasamy, S. K., and R. G. Larson. 2004. Binding and insertion of α-helical anti-microbial peptides in POPC bilayers studied by molecular dynamics simulations. *Chem. Phys. Lipids.* 132:113–132.
5. Plenat, T., S. Boichot, P. Dosset, P.-E. Milhiet, and C. Le Grimellec. 2005. Coexistence of a two-states organization for a cell-penetrating peptide in lipid bilayer. *Biophys. J.* 89:4300–4309.
6. Kasbauer, M., and T. M. Bayerl. 1999. Formation of domains of cationic or anionic lipids in binary lipid mixtures increases the electrostatic coupling strength of water-soluble proteins to supported bilayers. *Biochemistry.* 38:15258–15263.
7. Sackmann, E. 1996. Supported membranes: scientific and practical applications. *Science.* 71:43–48.
8. Tanaka, M., and E. Sackmann. 2005. Polymer-supported membranes as models of the cell surface. *Nature.* 437:656–663.
9. Bagatolli, L. A., and E. Gratton. 2000. Two photon fluorescence microscopy of coexisting lipid domains in giant unilamellar vesicles of binary phospholipid mixtures. *Biophys. J.* 78:290–305.
10. Arbuzova, A., L. Wang, J. Wang, G. Hangyas-Mihalyne, D. Murray, B. Honig, and S. McLaughlin. 2000. Membrane binding of peptides containing both basic and aromatic residues. Experimental studies with peptides corresponding to the scaffolding region of caveolin and the effector region of MARCKS. *Biochemistry.* 39:10330–10339.
11. Menger, F. M., and M. I. Angelova. 1998. Giant vesicles: imitating the cytological processes of cell membranes. *Acc. Chem. Res.* 31:789–797.
12. Hetzer, M., S. Heinz, S. Grage, and T. M. Bayerl. 1998. Asymmetric molecular friction in supported phospholipid bilayers revealed by NMR measurements of lipid diffusion. *Langmuir.* 14:982–984.
13. Kasbauer, M., M. Junglas, and T. M. Bayerl. 1999. Effect of cationic lipids in the formation of asymmetries in supported bilayers. *Biophys. J.* 76:2600–2605.
14. Richter, R. P., N. Maury, and A. R. Brisson. 2005. On the effect of the solid support on the interleaflet distribution of lipids in supported lipid bilayers. *Langmuir.* 21:299–304.
15. Xie, A. F., R. Yamada, A. A. Gewirth, and S. Granick. 2002. Materials science of the gel to fluid phase transition in a supported phospholipid bilayer. *Phys. Rev. Lett.* 89:246103/246101–246103/246104.
16. Leonard, A., C. Escrive, M. Laguerre, E. Pebay-Peyroula, W. Neri, T. Pott, J. Katsaras, and E. J. Dufourc. 2001. Location of cholesterol in DMPC membranes. A comparative study by neutron diffraction and molecular mechanics simulation. *Langmuir.* 17:2019–2030.
17. Rinia, H. A., J.-W. P. Boots, D. T. S. Rijkers, R. A. Kik, M. M. E. Snel, R. A. Demel, J. A. Killian, J. P. J. M. Van der Eerden, and

B. de Kruijff. 2002. Domain formation in phosphatidylcholine bilayers containing transmembrane peptides: specific effects of flanking residues. *Biochemistry*. 41:2814–2824.

18. Boon, J. M., and B. D. Smith. 2002. Chemical control of phospholipid distribution across bilayer membranes. *Med. Res. Rev.* 22:251–281.
19. Middelkoop, E., B. H. Lubin, E. M. Bevers, J. A. Op den Kamp, P. Comfurius, D. T. Chiu, R. F. Zwaal, L. L. van Deenen, and B. Roelofsen. 1988. Studies on sickled erythrocytes provide evidence that the asymmetric distribution of phosphatidylserine in the red cell membrane is maintained by both ATP-dependent translocation and interaction with membrane skeletal proteins. *Biochim. Biophys. Acta*. 937:281–288.
20. Lin, W.-C., C. D. Blanchette, T. V. Ratto, and M. L. Longo. 2006. Lipid asymmetry in DLPC/DSPC-supported lipid bilayers: a combined AFM and fluorescence microscopy study. *Biophys. J.* 90:228–237.
21. Seigneuret, M., A. Zachowski, A. Hermann, and P. F. Devaux. 1984. Asymmetric lipid fluidity in human erythrocyte membrane: new spin-label evidence. *Biochemistry*. 23:4271–4275.
22. Chahine, J. M. E. H., S. Cribier, and P. F. Devaux. 1993. Phospholipid transmembrane domains and lateral diffusion in fibroblasts. *Proc. Natl. Acad. Sci. USA*. 90:447–451.
23. Devaux, P. F., and R. Morris. 2004. Transmembrane asymmetry and lateral domains in biological membranes. *Traffic*. 5:241–246.
24. Pike, L. J. 2003. Lipid rafts: bringing order to chaos. *J. Lipid Res*. 44: 655–667.
25. Veatch, S. L., and S. L. Keller. 2003. Separation of liquid phases in giant vesicles of ternary mixtures of phospholipids and cholesterol. *Biophys. J*. 85:3074–3083.
26. Simons, K., and E. Ikonen. 1997. Functional rafts in cell membranes. *Nature*. 387:569–572.
27. Silvius, J. R. 2003. Role of cholesterol in lipid raft formation: lessons from lipid model systems. *Biochim. Biophys. Acta*. 1610:174–183.
28. Varma, R., and S. Mayor. 1998. GPI-anchored proteins are organized in submicron domains at the cell surface. *Nature*. 394:798–801.
29. Jacobson, K., E. D. Sheets, and R. Simson. 1995. Revisiting the fluid mosaic model of membranes. *Science*. 268:1441–1442.
30. McMahon, H. T., and I. G. Mills. 2004. COP and clathrin-coated vesicle budding: different pathways, common approaches. *Curr. Opin. Cell Biol*. 16:379–391.
31. Maxfield, F. R., and I. Tabas. 2005. Role of cholesterol and lipid organization in disease. *Nature*. 438:612–621.
32. Hinderliter, A., P. F. F. Almeida, C. E. Creutz, and R. L. Biltonen. 2001. Domain formation in a fluid mixed lipid bilayer modulated through binding of the C2 protein motif. *Biochemistry*. 40:4181–4191.
33. Simons, K., and R. Ehehalt. 2002. Cholesterol, lipid rafts, and disease. *J. Clin. Invest*. 110:597–603.
34. Denisov, G., S. Wanaski, P. Luan, M. Glaser, and S. McLaughlin. 1998. Binding of basic peptides to membranes produces lateral domains enriched in the acidic lipids phosphatidylserine and phosphatidylinositol 4,5-bisphosphate: an electrostatic model and experimental results. *Biophys. J*. 74:731–744.
35. Franzin, C. M., and P. M. Macdonald. 2001. Polylysine-induced ^{2}H NMR-observable domains in phosphatidylserine/phosphatidylcholine lipid bilayers. *Biophys. J*. 81:3346–3362.
36. Poveda, J. A., J. A. Encinar, A. M. Fernandez, C. R. Mateo, J. A. Ferragut, and J. M. Gonzalez-Ros. 2002. Segregation of phosphatidic acid-rich domains in reconstituted acetylcholine receptor membranes. *Biochemistry*. 41:12253–12262.
37. May, S., D. Harries, and A. Ben-Shaul. 2000. Lipid demixing and protein-protein interactions in the adsorption of charged proteins on mixed membranes. *Biophys. J*. 79:1747–1760.
38. Gil, T., J. H. Ipsen, O. G. Mouritsen, M. C. Sabra, M. M. Sperotto, and M. J. Zuckermann. 1998. Theoretical analysis of protein organization in lipid membranes. *Biochim. Biophys. Acta*. 1376:245–266.
39. Yaroslavov, A. A., A. A. Efimova, V. I. Lobyshev, and V. A. Kabanov. 2002. Reversibility of structural rearrangements in the negative vesicular membrane upon electrostatic adsorption/desorption of the polycation. *Biochim.Biophys. Acta*. 1560:14–24.
40. McLaughlin, S., and D. Murray. 2005. Plasma membrane phosphoinositide organization by protein electrostatics. *Nature*. 438: 605–611.
41. Epand, R. M. 2004. Do proteins facilitate the formation of cholesterol-rich domains? *Biochim. Biophys. Acta*. 1666:227–238.
42. Hinderliter, A., R. L. Biltonen, and P. F. F. Almeida. 2004. Lipid modulation of protein-induced membrane domains as a mechanism for controlling signal transduction. *Biochemistry*. 43:7102–7110.
43. Fukushima, K., Y. Muraoka, T. Inoue, and R. Shimozawa. 1989. Conformational study of poly(L-lysine) interacting with acidic phospholipid vesicles. *Biophys. Chem*. 34:83–90.
44. Hammes, G. G., and S. E. Schullery. 1970. Structure of macromolecular aggregates. II. Construction of model membranes from phospholipids and polypeptides. *Biochemistry*. 9:2555–2563.
45. Carrier, D., and M. Pezolet. 1986. Investigation of polylysine-dipalmitoylphosphatidylglycerol interactions in model membranes. *Biochemistry*. 25:4167–4174.
46. Laroche, G., D. Carrier, and M. Pezolet. 1988. Study of the effect of poly(L-lysine) on phosphatidic acid and phosphatidylcholine/phosphatidic acid bilayers by Raman spectroscopy. *Biochemistry*. 27:6220–6228.
47. Liu, F., N. A. H. Lewis Ruthven, S. Hodges Robert, and N. McElhaney Ronald. 2002. Effect of variations in the structure of a polyleucine-based alpha-helical transmembrane peptide on its interaction with phosphatidylcholine bilayers. *Biochemistry*. 41:9197–9207.
48. Liu, F., R. N. A. H. Lewis, R. S. Hodges, and R. N. McElhaney. 2004. Effect of variations in the structure of a polyleucine-based α-helical transmembrane peptide on its interaction with phosphatidylethanolamine bilayers. *Biophys. J*. 87:2470–2482.
49. Menger, F. M., V. A. Seredyuk, M. V. Kitaeva, A. A. Yaroslavov, and N. S. Melik-Nubarov. 2003. Migration of poly-L-lysine through a lipid bilayer. *J. Am. Chem. Soc*. 125:2846–2847.
50. Yaroslavov, A. A., O. E. Kuchenkova, I. B. Okuneva, N. S. Melik-Nubarov, N. O. Kozlova, V. I. Lobyshev, F. M. Menger, and V. A. Kabanov. 2003. Effect of polylysine on transformations and permeability of negative vesicular membranes. *Biochim. Biophys. Acta*. 1611:44–54.
51. Reviakine, I., A. Simon, and A. Brisson. 2000. Effect of Ca^{2+} on the morphology of mixed DPPC-DOPS supported phospholipid bilayers. *Langmuir*. 16:1473–1477.
52. Richter, R., A. Mukhopadhyay, and A. Brisson. 2003. Pathways of lipid vesicle deposition on solid surfaces: a combined QCM-D and AFM study. *Biophys. J*. 85:3035–3047.
53. Jass, J., T. Tjarnhage, and G. Puu. 2000. From liposomes to supported, planar bilayer structures on hydrophilic and hydrophobic surfaces: an atomic force microscopy study. *Biophys. J*. 79:3153–3163.
54. McConnell, H. M., T. H. Watts, R. M. Weis, and A. A. Brian. 1986. Supported planar membranes in studies of cell-cell recognition in the immune system. *Biochim. Biophys. Acta*. 864:95–106.
55. Feng, Z. V., T. A. Spurlin, and A. A. Gewirth. 2005. Direct visualization of asymmetric behavior in supported lipid bilayers at the gel-fluid phase transition. *Biophys. J*. 88:2154–2164.
56. Keller, D., N. B. Larsen, I. M. Moeller, and O. G. Mouritsen. 2005. Decoupled phase transitions and grain-boundary melting in supported phospholipid bilayers. *Phys. Rev. Lett*. 94:025701/025701–025701/025704.
57. Yang, J., and J. Appleyard. 2000. The main phase transition of mica-supported phosphatidylcholine membranes. *J. Phys. Chem. B*. 104: 8097–8100.
58. Silvius, J. R. 1982. Thermotropic Phase Transitions of Pure Lipids in Model Membranes and Their Modifications by Membrane Proteins. John Wiley & Sons, New York.
59. Leonenko, Z. V., E. Finot, H. Ma, T. E. S. Dahms, and D. T. Cramb. 2004. Investigation of temperature-induced phase transitions in DOPC

and DPPC phospholipid bilayers using temperature-controlled scanning force microscopy. *Biophys. J.* 86:3783–3793.

60. Garcia-Manyes, S., G. Oncins, and F. Sanz. 2005. Effect of temperature on the nanomechanics of lipid bilayers studied by force spectroscopy. *Biophys. J.* 89:4261–4274.
61. Polyansky, A. A., P. E. Volynsky, D. E. Nolde, A. S. Arseniev, and R. G. Efremov. 2005. Role of lipid charge in organization of water/lipid bilayer interface: insights via computer simulations. *J. Phys. Chem. B.* 109:15052–15059.
62. You, H., and L. Yu. 1998. Nano-deposition of protein molecules using tapping-mode atomic force microscopy: facts or artifacts. *Probe Microscopy.* 1:233–237.
63. Leonenko, Z. V., D. Merkle, S. P. Lees-Miller, and D. T. Cramb. 2002. Lipid phase dependence of DNA-cationic phospholipid bilayer interactions examined using atomic force microscopy. *Langmuir.* 18:4873–4884.
64. Costigan, S. C., P. J. Booth, and R. H. Templer. 2000. Estimations of lipid bilayer geometry in fluid lamellar phases. *Biochim. Biophys. Acta.* 1468:41–54.
65. Liu, F., N. A. H. Lewis Ruthven, S. Hodges Robert, and N. McElhaney Ronald. 2004. Effect of variations in the structure of a polyleucine-based alpha-helical transmembrane peptide on its interaction with phosphatidylethanolamine bilayers. *Biophys. J.* 87:2470–2482.
66. Mecke, A., D.-K. Lee, A. Ramamoorthy, B. G. Orr, and M. M. Banaszak Holl. 2005. Synthetic and natural polycationic polymer nanoparticles interact selectively with fluid-phase domains of DMPC lipid bilayers. *Langmuir.* 21:8588–8590.
67. Richter, R. P., and A. R. Brisson. 2005. Following the formation of supported lipid bilayers on mica: a study combining AFM, QCM-D, and ellipsometry. *Biophys. J.* 88:3422–3433.
68. Shibata, A., S. Murata, S. Ueno, S. Liu, S. Futaki, and Y. Baba. 2003. Synthetic copoly(Lys/Phe) and poly(Lys) translocate through lipid bilayer membranes. *Biochim. Biophys. Acta.* 1616:147–155.
69. Rossetti, F. F., I. Reviakine, G. Csucs, F. Assi, J. Voeroes, and M. Textor. 2004. Interaction of poly(L-lysine)-g-poly(ethylene glycol) with supported phospholipid bilayers. *Biophys. J.* 87:1711–1721.
70. Wiegand, G., N. Arribas-Layton, H. Hillebrandt, E. Sackmann, and P. Wagner. 2002. Electrical properties of supported lipid bilayer membranes. *J. Phys. Chem. B.* 106:4245–4254.
71. Raedler, J., H. Strey, and E. Sackmann. 1995. Phenomenology and kinetics of lipid bilayer spreading on hydrophilic surfaces. *Langmuir.* 11:4539–4548.
72. Steinem, C., A. Janshoff, W. P. Ulrich, M. Sieber, and H. J. Galla. 1996. Impedance analysis of supported lipid bilayer membranes: a scrutiny of different preparation techniques. *Biochim. Biophys. Acta.* 1279:169–180.
73. Diederich, A., G. Baehr, and M. Winterhalter. 1998. Influence of polylysine on the rupture of negatively charged membranes. *Langmuir.* 14:4597–4605.